

# Anomalous separations of the CMB temperature angular power spectrum

Md Ishaque Khan<sup>1,\*</sup>; Rajib Saha<sup>2,†</sup>

<sup>1,2</sup>Department of Physics, Indian Institute of Science Education and Research (IISER), Bhopal 462066, India

## Abstract

In this article, we propose a novel technique to test for anomalous features in the CMB. We analyse separations of the observed CMB angular power spectrum ( $C_\ell$ ) using temperature anisotropy data from WMAP 9 year ILC and 2018 Planck maps of Commander, NILC and SMICA. We estimate the minimum, maximum, average separations and ratios of the maximum to minimum separations between consecutive multipoles of the weighted spectrum,  $f(\ell)C_\ell$ . We see that such  $f(\ell)$ 's with higher multipole powers mitigate the parity asymmetry anomaly. For anomalous separations, we find that data exhibits anomalous ranges of multipoles defined by different  $\ell_{max}$  and  $\ell_{min}$  values, specifically for the entire range of multipoles from 2 – 31 of this work. Without parity based distinctions, most significantly, the maximum separation of the range  $8 \leq \ell \leq 31$  is seen to be anomalously low at the 99.93% confidence level for  $f(\ell) = \ell$  (WMAP),  $\frac{\ell(\ell+1)}{2\pi}$  (Planck NILC), the latter indicating a strong deviation from the Sachs-Wolfe plateau for maximum separations among low multipoles. The analysis is repeated for odd and even multipoles taken separately, in the same multipole ranges. Most noticeably, the even multipoles are seen to have anomalously low maximum and average separations relative to their odd counterparts, the most outstanding among which is the anomalously low maximum separation for even multipoles in the range  $6 \leq \ell \leq 31$  for  $f(\ell) = \ell$  (WMAP), at the 99.77% confidence level. For separation ratios, the multipole ranges are similar to those which turn up as anomalous when only separations are considered.

**Keywords**— cosmic background radiation – inflation – methods: data analysis – cosmology: miscellaneous

## 1 Introduction

Cosmological data analysis in the past unveiled many anomalies in the observed Cosmic Microwave Background (CMB) patterns of WMAP [12] and Planck [37] satellite missions. It has hence become imperative to study anomalies in both WMAP and Planck maps to make discrepancies more discernible if any such exist. Such anomalies include the north-south power asymmetry [5], the anomalous cold spot ([40], [14], [13]), high degree of octupole-quadrupole alignment ([39], [17], [38]), quadrupole power deficit ([4], [24]) and planarity of the octupole [16], and the like. Some of the latter ones concerning the quadrupole and octupole have been somewhat mitigated using a hypothetical foreground reduction [1].

Anomalies, specifically those of the power excess for lower odd multipoles [30], have been shown to be a part of a more general trend in the observed maps ([29], [3], [42]) referred to as a ‘parity asymmetry’ of the power distributed among low odd and even parity multipoles. Studies of the Integrated Sachs-Wolfe (ISW) effect for low multipoles [15] help explain the power deficit in this range of multipoles. [22] show how an ISW foreground subtraction helps obscure the anomalous effects of the quadrupole and its alignment with the octupole. Besides, modifications to the scale of the primordial power ([26], [8], [23]) may serve as a starting point for explaining the ‘parity asymmetry’ and other power deficit anomalies. An excellent propo-

sition of a Finsler spacetime [9] also helps naturally explain parity asymmetry.

Probes of anomalies till now have delved into low multipole ranges in the observational data. Large scale or low multipole studies of CMB data have become imperative for various reasons as explained by [12]. Our analyses presented here also show that such ranges are distinctively anomalous relative to the theoretical  $\Lambda$ CDM temperature power spectrum.

We propose a novel analysis of separations or absolute differences between consecutive CMB temperature angular power spectrum (APS) measures ( $C_\ell$ 's). We investigate anomalous maximum, minimum and average separations, for low multipoles, by using a weighted APS ( $f(\ell)C_\ell$ ). We analyse not just all multipoles, but also even and odd multipoles taken distinctly. This helps understand the behaviour of parity preference of the APS. We also look for anomalous ratios of maximum to minimum separations.

Our paper is organised as follows : Section 2 states the basic framework of the analysis presented thereafter. Section 3 describes our way of testing consecutive multipole separations with simulations. We report anomalies in section 4, for all multipole and for even/odd multipole separations, respectively. In section 5, we summarise the most significant results for anomalous separations. In section 6, we present anomalous ratios of the maximum to minimum separations. In section 7, we present our tests of parity asymmetry with six  $f(\ell)$ 's and use the results to further substantiate our argument for the choices of these  $f(\ell)$ 's when testing for anomalous separations. And, in section 8,

\*email: ishaque16@iiserb.ac.in

†email: rajib@iiserb.ac.in

we deduce any general trends in anomalies based on our results and opine on apparent discrepancies.

## 2 Estimators

The Cosmic Microwave Background (CMB) provides a measure of temperature anisotropies relative to the uniform mean background temperature of nearly  $2.726K$  [21]. These anisotropies are denoted by  $\Delta T(\hat{n})$ , where  $\hat{n}$  defines a direction in the CMB sky specifically given in terms of  $(\theta, \phi)$  in spherical polar coordinates with the radius of the last scattering surface. The unbiased angular power spectrum estimator is given by  $C_\ell$ 's as [27]:

$$C_\ell = \frac{1}{2\ell + 1} \sum_{m=-\ell}^{\ell} |a_{\ell m}|^2, \quad (1)$$

where, the  $a_{\ell m}$ 's are coefficients of the expansion:

$$\Delta T(\hat{n}) = \sum_{\ell=1}^{\infty} \sum_{m=-\ell}^{\ell} a_{\ell m} Y_{\ell m}(\hat{n}). \quad (2)$$

Hence one may ascribe units of  $(\mu K)^2$  to the  $C_\ell$ 's.

In this article, we present a new idea of investigating CMB temperature angular power spectrum anomalies. We propose a novel set of estimators for this purpose, based on the CMB angular power spectrum of the observed CMB maps. More specifically, we seek to realise nearest neighbour spacings in the context of CMB angular power spectral measures ( $C_\ell$ 's). Such estimators have not been spoken of in existing literature but can be understood in terms of the absolute differences or separations between any two consecutive  $C_\ell$ 's.

For a given range of multipoles  $[\ell_{min}, \ell_{max} + 1]$ , the separations between consecutive  $C_\ell$ 's were estimated, weighted by  $f(\ell)$ 's. Say, such consecutive multipole separations of  $f(\ell)C_\ell$ 's are  $[\Delta_1, \Delta_2, \dots]$ , then four estimators to detect anomalies are as follows:

$$\begin{aligned} max_i &= max[\Delta_1^i, \Delta_2^i, \dots], \\ min_i &= min[\Delta_1^i, \Delta_2^i, \dots], \\ avg_i &= \frac{\Delta_1^i + \Delta_2^i + \dots}{N}, \\ r_i &= \frac{max_i}{min_i}, \end{aligned} \quad (3)$$

which stand for the maximum, minimum, average of a set of separations and the ratio of the maximum to minimum separations, respectively. Here,  $i = a, o, e$ , where  $a, o, e$  stand for all, odd and even multipoles, and  $N =$  number of separations for a given range of  $\ell$ 's.

These estimators have been proposed here as exhaustive probes of anomalous separations, because the lower and upper limits ( $\ell_{min}, \ell_{max}$  respectively) of a multipole range have also been varied appropriately for all the analyses. Being extreme statistical measures, these estimators (excluding the average measure) represent rare occurrences of certain values of the nearest neighbour separations, yet

along with the average or mean separation and the ratio of the maximum to minimum of a multipole range, these, will characterise anomalous behaviours of separations in an easily quantifiable way.

We present anomalies for all, odd and even multipole separations for four simple cases of  $f(\ell) = 1, \frac{\ell(\ell+1)}{2\pi}, \ell, \ell^2$ . For reference purposes we have included the plots of the four  $f(\ell)C_\ell$ 's with multipoles in figure 1. Fractional powers of multipoles in  $f(\ell)$  are also possible choices, but such choices and arguments in favour of those will be postponed for future work.

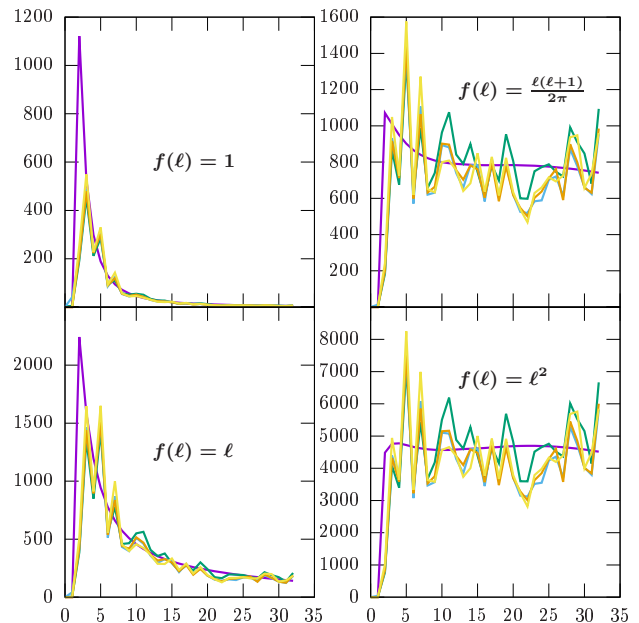


Figure 1:  $f(\ell)C_\ell$  versus  $\ell$ , the weighted angular power spectrum : The plot compares the theoretical best fit to Planck (purple) with COMB (green), NILC (light blue), SMICA (ochre) and WMAP (yellow) maps used here, all equivalently with zero smoothing but with a pixel window application appropriate for  $n_{side} = 16$

## 3 Methodology

We have estimated discrepancies relative to the theoretical APS (Planck 2018 best fit) with the help of the HEALPix [25] package, by considering  $10^4$  simulations of the theoretical temperature angular power spectrum to account for statistical fluctuations while studying the minimum, maximum and average of the separations between consecutive  $f(\ell)C_\ell$ 's.

Observed data maps used here for probing anomalous separations are: WMAP 9 year ILC and 2018 release full mission Planck Commander (COMB), NILC and SMICA maps from latest sources: [33] and [19]. These have been downgraded with the help of HEALPix [25] software facilities to a HEALPix  $n_{side} = 16, n_{\ell_{max}} = 32$  (hence, an appropriate pixel\_window) with no beam smoothing ( $fwhm\_arcmin = 0.0d0$ ) and the simulations are obtained using the same resolution. With all data maps, the theoretical power spectrum, and simulations thereof on an equal footing, we have proceeded with the analysis. We

have excluded multipoles  $\ell = 0, 1$  as these correspond respectively to the monopole of uniform CMB temperature ( $\approx 2.726K$ ) [21], and the dipole which arises due to our peculiar motion relative to the CMB rest frame [7].

We have taken minimum, maximum and average of the separations of  $f(\ell)C_\ell$ 's for consecutive multipoles firstly without any distinction between odd or even ones and later separately for odd/even multipoles to study anomalies that arise upon such parity based distinctions. Here, a separation means the absolute value of the difference between two consecutive  $f(\ell)C_\ell$ 's. For example, for the 6 multipoles in the range [2, 7], we have 5 separations with no parity based distinction namely,  $|f(2)C_2 - f(3)C_3|, |f(3)C_3 - f(4)C_4|, \dots, |f(6)C_6 - f(7)C_7|$ . Whereas for even and odd multipoles taken distinctly, in the same range, we have 2 separations each for even and odd multipoles namely,  $|f(2)C_2 - f(4)C_4|, |f(4)C_4 - f(6)C_6|$  and  $|f(3)C_3 - f(5)C_5|, |f(5)C_5 - f(7)C_7|$  respectively.

For characterising the extent to which a separation may be anomalous in a quantitative way, we define the following probabilities:

$$\begin{aligned} \text{s-value} & : P^t(x), \\ \text{p-value} & : P^b(x) = 1 - P^t(x), \\ \text{where,} & \\ x & = (\min_i, \max_i, \text{avg}_i, r_i), \\ i & = a, o, e, \end{aligned} \quad (4)$$

and  $a, o, e$  as before, stand for all (no parity based distinction), odd and even multipoles respectively.

$P^t(x)$  (hereafter referred to as the 's-value') is the probability of the theoretical spectrum having a value greater than a data map for the four entities, that are, the minimum, maximum, average separation and the ratio of the maximum to minimum separations, respectively, denoted by  $x$ . This is calculated by counting the number of errant simulations having these entities greater than the observed map and dividing the number by the total number of simulations, that being  $10^4$  throughout this paper.

$P^b(x)$  (or the familiar 'p-value') is similarly defined as the probability of simulations having a value of the quantity  $x$  less than that from observational data. Probability plots for  $P^b$  are in log-scale along the vertical axis. Plots for  $P^t$  are not in log-scale. All probability plots mention 0.05, 0.95 (in dotted red lines) corresponding to the 5%–95% confidence range of hypothesis testing methodology ([6], [20], [35], [34]). Therefore all probabilities which feature below 5% or above 95% have been reported here. A considerable discourse against usage of such confidence intervals is given by [32] or that against the often assumed complementarity of the s- and p-values is presented in the work of [41].

As may be intuitively obvious from figure 1, the maximum and minimum separations for  $f(\ell)C_\ell$ 's may lie in any of the lower or higher multipole ranges and hence it becomes necessary to scan the multipole ranges by changing not only the upper bound of the multipole range ( $\ell_{max}$ , whilst keeping the lower bound fixed), but also the lower bound ( $\ell_{min}$ , whilst keeping the upper bound fixed). Also considering not just the minimum and maximum separa-

tions, but also computing the average value of a set of separations for a given  $\ell_{max}$  or  $\ell_{min}$  for the same reason, is needed.

We have, therefore, calculated the maximum, minimum and average separations by varying  $\ell_{max}$ 's and  $\ell_{min}$ 's. So, for example, multipoles in the range [2, 7] will correspond to an  $\ell_{max} = 6$  where the  $\ell_{min}$  is fixed at  $\ell_{min} = 2$ . A similar scheme holds for the  $\ell_{min}$ 's which have been varied keeping  $\ell_{max}$  fixed at  $\ell_{max} = 30$ .  $\ell = 0, 1$  have already been excluded for reasons aforementioned. Also having a maximum upper limit of  $\ell_{max} = 30$ , implies that we are looking for anomalies in the range [2, 31]. This invariably means that multipole  $\ell = 32$  is excluded from our analysis. This is because, although including  $\ell = 32$  would not have affected our results for all separations (no parity distinctions), but, when we scan for anomalies after taking odd and even multipole separations distinctly, we should have an equal number of odd and even separations for any chosen range of multipoles.

Hence with this forethought,  $\ell = 32$  is excluded not only for the analysis with parity based distinction but also when all multipoles are treated without distinction, so that comparisons of results between the two analyses later on seem legitimate. This is ensured further by choosing only even numbers for  $\ell_{min}$ 's and  $\ell_{max}$ 's. Thus,  $\ell_{max}$ 's have been varied from  $6 \rightarrow 30$  (by fixing  $\ell_{min} = 2$ ) in steps of  $\Delta\ell = 2$  for all separations and  $\ell_{min}$ 's have been varied from  $2 \rightarrow 26$  (having fixed  $\ell_{max} = 30$ ) in steps of  $\Delta\ell = 2$  for all separations. Similar variations of  $\ell_{min}$  and  $\ell_{max}$  have been made for odd and even multipole separations when those are considered individually, but those are varied in steps of  $\Delta\ell = 4$  for, that being the most sensible choice, keeps at least two separations of odd and even multipoles for comparison when maximum and minimum among the set of separations for a given  $\ell_{max}$  or  $\ell_{min}$  are computed.

## 4 Results: Separations

We present the  $\ell_{min}$  or  $\ell_{max}$  ranges of the four CMB temperature anisotropy data sources which are anomalous along with their respective probabilities  $P^t$  and/or  $P^b$ .

### 4.1 All multipoles in [2, 31]

For the entire set of multipoles in [2, 31], the anomalous separations are presented here.

#### 4.1.1 $f(\ell) = 1$

When considering all separations, anomalies arise when  $\ell_{min}$  is varied for all four maps. For a variation of  $\ell_{max}$  however, only WMAP shows anomalies (See figure 2). The most anomalous case for COMM is for  $\ell_{min} = 8$  where the p-value of the average separation is only about 6.3 in 1000, and for the maximum separation, it is for  $\ell_{min} = 16, 22$  and the p-value is 3.87 and 1.53 in 100 respectively. For NILC, the most significant is  $\ell_{min} = 8$  with an s-value of 99.29% for the maximum separation; others are  $\ell_{min} = 12, 20, 22$  with lesser significant values.

For average separation (NILC) the most anomalous is again  $\ell_{min} = 8$  with a p-value of 1.54 in 100 parts, while the others are  $\ell_{min} = 12, 18, 20, 22$  with lesser significant values. For SMICA, the most anomalous is  $\ell_{min} = 8$  for both average and maximum separations, with the s-value higher than SMICA being 99.26% for maximum, and, 99.23% for average separations. Other anomalous multipole separations with lesser significance are for  $\ell_{min} = 12, 20$  for the maximum separation, and  $\ell_{min} = 12, 20, 22$  for the average separation, respectively, for SMICA. Similarly for WMAP we have for  $\ell_{min} = 24$  for minimum separation an s-value of 96.79%, and for both maximum and average separations, it is for  $\ell_{min} = 8$  with s-values of 99.13% and 99.55% respectively. Also, WMAP shows maximally anomalous  $\ell_{max} = 24$  for minimum separation with an s-value of 97.36%, whilst other maps do not show anomalies for  $\ell_{max}$ 's. Other anomalous ones for WMAP for minimum separation are  $\ell_{max} = 26, 28$ .

#### 4.1.2 $f(\ell) = \frac{\ell(\ell+1)}{2\pi}$

In this case too, anomalies arise mainly for variations of  $\ell_{min}$  for all four maps, save NILC, which also shows anomalies for certain  $\ell_{max}$ 's (See figure 3). For COMM, there is an entire range of values of  $\ell_{min} = 6 \rightarrow 16$  which is anomalous for the maximum and average separations. The most significant is  $\ell_{min} = 8$  again, with p-values of 1.2 in 1000 parts for the maximum and 8.9 in 1000 for the average separations. NILC has an anomalous range of  $\ell_{max} = 14 \rightarrow 18$  for the minimum separation, with  $\ell_{max} = 14$  being most significant with an s-value of 96.75%.  $\ell_{min} = 8 \rightarrow 16$  is anomalous for the maximum separation with highest s-value of 99.93% for  $\ell_{min} = 8$  for NILC.  $\ell_{min} = 6 \rightarrow 14, 18 \rightarrow 22$  are anomalous for average separations in NILC with maximum s-value for  $\ell_{min} = 8$ , which is 99.7%. For SMICA the anomalous ranges are  $\ell_{min} = 8 \rightarrow 12$  for maximum separation and  $\ell_{min} = 6 \rightarrow 14$  for average separation. The most significant is  $\ell_{min} = 8$  again for both kinds of separations, with p-values of 8.2 and 4 in 1000 for maximum and average separations respectively. For WMAP, again the most significant is  $\ell_{min} = 8$  for both maximum and average separations. The s-values of WMAP for these are 99.59% and 99.55% respectively.

#### 4.1.3 $f(\ell) = \ell$

For this case similarly, mostly for  $\ell_{min}$  variations, anomalous ranges are found for all four maps. Only WMAP shows an anomaly for  $\ell_{max} = 6$  (See figure 4). COMM with  $\ell_{min} = 12$  for maximum separations has highest s-value of 99.23% whereas others of lesser significance are  $\ell_{min} = 8, 14, 16$ ;  $\ell_{min} = 8$  for average separation has the highest s-value of 99.67%, while others with lower s-values are  $\ell_{min} = 6, 10, 12$ . NILC with  $\ell_{min} = 8$  for both maximum and average separations is most anomalous with p-values of 2.8 and 5.6 in 1000 parts respectively. Other anomalous ranges for NILC are  $\ell_{min} = 10, 12, 18, 20$  for the maximum separation and  $\ell_{min} = 10, 12, 18, 20, 22$  for the average separation. SMICA similarly reveals that  $\ell_{min} = 8$  is most anomalous for both maximum and aver-

age separations with p-values of 1.4 and 2.8 in 1000 respectively. Other lesser significant anomalous ones for SMICA are  $\ell_{min} = 10, 12, 14, 18$  for the maximum separation and  $\ell_{min} = 10, 12, 20$ . Also for WMAP, the most anomalous is  $\ell_{min} = 8$  for maximum and average separations with considerable p-values of 7 in 10,000 and 2.2 in 1000. WMAP also shows an anomalous  $\ell_{max} = 6$  with a p-value of 3.07 in 100 for the minimum separation.

#### 4.1.4 $f(\ell) = \ell^2$

In this case, COMM and SMICA show some nearly insignificant anomalous  $\ell_{max}$ 's but as usual all four maps show anomalous ranges of  $\ell_{min}$ 's. (See figure 5). Starting with COMM again,  $\ell_{max} = 22$  for the minimum separation has an s-value for COMM of 95.27%, whereas again the highest s-values are for  $\ell_{min} = 8$  for the maximum and average separations of 99.83% and 99.09% respectively. Other anomalous ranges for COMM are  $\ell_{min} = 16, 18, 20$  for the minimum separation,  $\ell_{min} = 6 \rightarrow 16$  for the maximum separation and  $\ell_{min} = 6 \rightarrow 16, 20$  for the average separation. Again for NILC too,  $\ell_{min} = 8$  is maximally anomalous with a considerable p-value of 9 in  $10^4$  parts and an s-value of 99.69% for the maximum and average separations. Other anomalous ranges for NILC are  $\ell_{min} = 10 \rightarrow 16$  for the maximum separation and  $\ell_{min} = 6 \rightarrow 22$  for the average separation. For  $\ell_{max} = 10$  SMICA is anomalous with an s-value of 96.05% for the minimum separation.  $\ell_{min} = 8$  is again maximally anomalous for SMICA with s-values of 98.86% and 99.58% for the maximum and average separations, while other anomalous multipoles are given by  $\ell_{min} = 10, 12$  for the maximum separation and  $\ell_{min} = 6 \rightarrow 14$  for the average separation. Similarly the highest s-values are 99.46% and 99.52% for the maximum and average separations for WMAP respectively for  $\ell_{min} = 8$ , while the other anomalous ranges are  $\ell_{min} = 10, 12, 14$  for the maximum separation and  $\ell_{min} = 10, 12, 20$  for the average separation.

## 4.2 Odd and even multipoles in [2, 31]

On treating  $f(\ell)C_\ell$ 's differently based on parity of the multipoles, some novel anomalies come up. For example, the minimum separation for a certain  $\ell_{max}$  or  $\ell_{min}$  shows anomalous behaviour in some ranges with a much greater significance relative to the case when all separations regardless of parity were being treated without distinction. Also many a time,  $f(\ell)C_\ell$ 's of a certain parity may only show up in anomalous ranges, whereas those of a different parity remain quiescent until the power to which the multipole in  $f(\ell)$  is raised is changed.

#### 4.2.1 $f(\ell) = 1$

Mostly the maximum and average separations in even multipoles (i.e.,  $max_e$  and  $avg_e$ ) show anomalous behaviour for all four maps, but at times, the minimum separation among odd multipoles ( $min_o$ ) also shows some anomalies (see figure 6).

COMM shows an anomaly for  $\ell_{max} = 10$ , for the minimum separation among odd multipoles ( $min_o$ ), with an

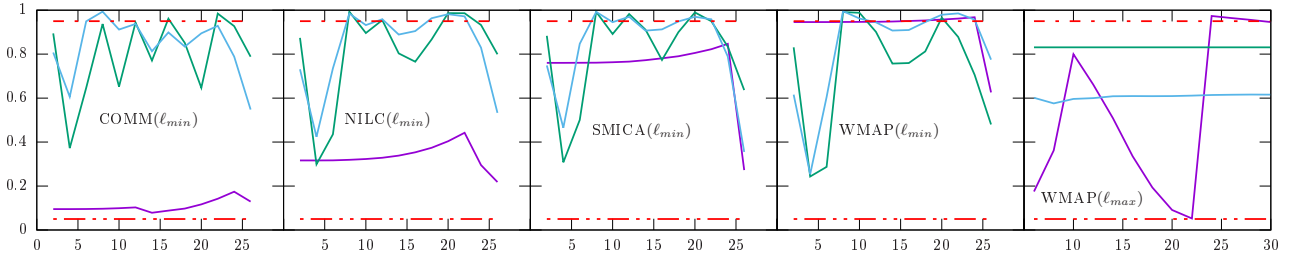


Figure 2: Probabilities  $P^t$  for  $min_a$ ,  $max_a$ ,  $avg_a$  (in purple, green and light blue, respectively) for  $f(\ell) = 1$  versus  $\ell_{max}$  or  $\ell_{min}$  as mentioned in parentheses () beside the name of the data map. Red dotted-dashed lines indicate 5% (double dots) and 95% (single dots).

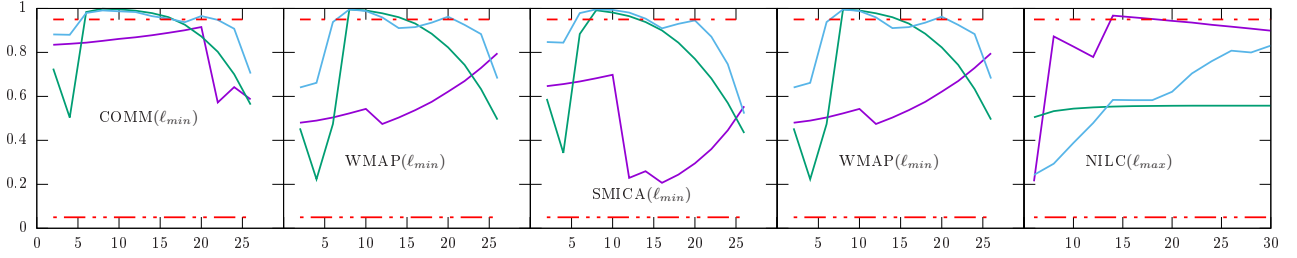


Figure 3: Probabilities  $P^t$  for  $min_a$ ,  $max_a$ ,  $avg_a$  (in purple, green and light blue, respectively) for  $f(\ell) = \frac{\ell(\ell+1)}{2\pi}$  versus  $\ell_{max}$  or  $\ell_{min}$  as mentioned in parentheses () beside the name of the data map. Red dotted-dashed lines indicate 5% (double dots) and 95% (single dots).

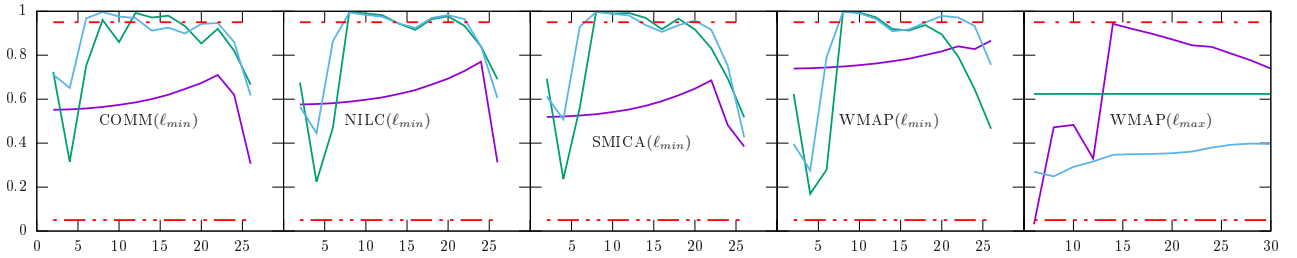


Figure 4: Probabilities  $P^t$  for  $min_a$ ,  $max_a$ ,  $avg_a$  (in purple, green and light blue, respectively) for  $f(\ell) = \ell$  versus  $\ell_{max}$  or  $\ell_{min}$  as mentioned in parentheses () beside the name of the data map. Red dotted-dashed lines indicate 5% (double dots) and 95% (single dots).

s-value of 97.76%. For the maximum and average separations among even multipoles, the entire range of  $\ell_{max}$ 's from  $\ell_{max} = 6 \rightarrow 30$  is anomalous with highest s-values of 98.06% for  $\ell_{max} = 10 \rightarrow 30$  for  $max_e$  and 99.51% for  $\ell_{max} = 26, 30$  for  $avg_e$ . For variations of  $\ell_{min}$ ,  $\ell_{min} = 2$  is the only anomalous one for both  $max_e$  and  $avg_e$  for COMM, with s-values of 98.06% and 99.51%.

For NILC, the entire range of  $\ell_{max} = 6 \rightarrow 30$  is anomalous for maximum and average separations among the even multipoles reaching the maximum s-values of 96.26% for  $\ell_{max} = 10 \rightarrow 30$  for  $max_e$ , and 99.16% for  $avg_e$  for  $\ell_{max} = 26, 30$ . Again, only for  $\ell_{min} = 2$ ,  $max_e$  is anomalous for NILC, with probability of 96.26%.  $\ell_{min} = 2, 6, 18, 22$  are anomalous for  $avg_e$  for NILC, but  $\ell_{min} = 2$  is most anomalous for  $avg_e$  with a probability of 99.16%.

Similarly for SMICA, the entire range of  $\ell_{max} = 6 \rightarrow 30$  is anomalous for both  $max_e$  and  $avg_e$ , with maximal probability of 96.96% for  $max_e$  for  $\ell_{max} = 10 \rightarrow 30$ , and that of 99.44% for  $\ell_{max} = 26, 30$  for  $avg_e$ .  $\ell_{max} = 26, 30$  are also anomalous for  $min_o$  for SMICA, with the

maximum s-value of 98.57% for  $\ell_{max} = 26$ . The range  $\ell_{min} = 2 \rightarrow 22$  is anomalous for  $min_o$  with a maximal probability of 98.58% for  $\ell_{min} = 22$  for SMICA.  $\ell_{min} = 2$  is anomalous for SMICA for  $max_e$  with a probability of 96.96%. Also  $\ell_{min} = 2, 18, 22$  are anomalous for  $avg_e$  with a maximal probability of 99.44% for  $\ell_{min} = 2$  for SMICA.

For WMAP,  $\ell_{max} = 14, 18$  are anomalous for  $min_o$  with  $\ell_{max} = 14$  being most anomalous with a probability of 98.01%. Again,  $\ell_{max} = 6 \rightarrow 30$  are all anomalous for  $max_e$  and  $avg_e$  for WMAP, with a maximal probability of 96.92% for  $\ell_{max} = 10 \rightarrow 30$  for  $max_e$ , and that of 99.16% for  $\ell_{max} = 26$  for  $avg_e$ . For  $\ell_{min}$  variations for WMAP, only  $\ell_{min} = 2$  is anomalous with a probability of 96.92% for  $max_e$  and 99.14% for  $avg_e$ .

#### 4.2.2 $f(\ell) = \frac{\ell(\ell+1)}{2\pi}$

For COMM, there are no anomalies except one for  $\ell_{min} = 6$  for the maximum separation of even multipoles which is almost insignificant with an s-value of 95.19%, hence prob-

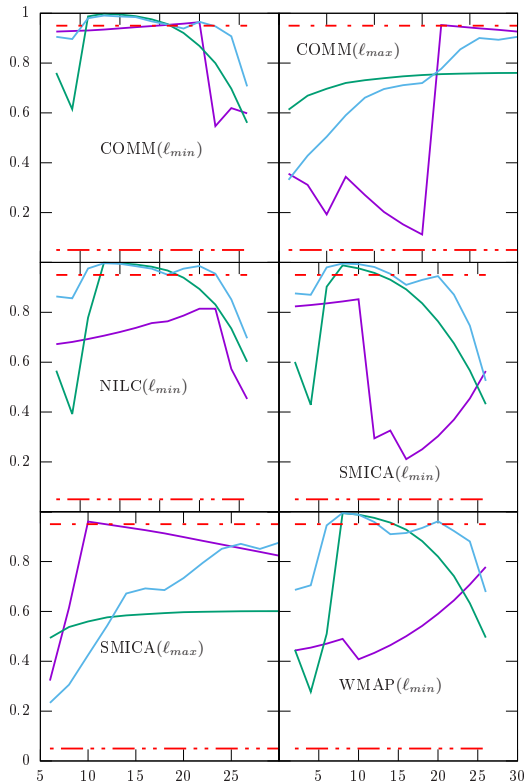


Figure 5: Probabilities  $P^t$  for  $min_a$ ,  $max_a$ ,  $avg_a$  (in purple, green and light blue, respectively) for  $f(\ell) = \ell^2$  versus  $\ell_{max}$  or  $\ell_{min}$  as mentioned in parentheses () beside the name of the data map. Red dotted-dashed lines indicate 5% (double dots) and 95% (single dots).

ability plots for COMM for  $\ell_{max}$  are not being presented here.

For the other plots, see figure 7. For  $\ell_{max}$  variations, only average separations of even multipoles reveal anomalous ranges, which are  $\ell_{max} = 22 \rightarrow 30$  for NILC,  $\ell_{max} = 18 \rightarrow 30$  for SMICA, and  $\ell_{max} = 14 \rightarrow 30$  for WMAP. Their maximum s-values are 97.17%, 97.86% and 99.50% for  $\ell_{max} = 26$  for the three maps.

For  $\ell_{min}$  variations,  $\ell_{min} = 6, 10, 14$  and  $\ell_{min} = 2, 6, 10$  are anomalous for  $max_e$  and  $avg_e$  for NILC, with maximum s-values of 98.43% for  $\ell_{min} = 10$  and 97.45% for  $\ell_{min} = 6$ , respectively. For SMICA,  $\ell_{min} = 10$  shows an anomaly with an s-value of 97.02% for  $max_o$ . For  $max_e$ ,  $\ell_{min} = 6, 10$  are anomalous with maximal s-value of 97.64% for  $\ell_{min} = 6$ , whereas for  $avg_e$ , for SMICA,  $\ell_{min} = 2, 6$  are anomalous with maximal s-value of 96.88% for  $\ell_{min} = 2$ . For WMAP,  $\ell_{min} = 6$  for  $max_e$  is anomalous with an s-value of 97.10%. Also,  $\ell_{min} = 2, 6, 10$  are anomalous for  $avg_e$  for WMAP, with a maximal s-value of 98.63% for  $\ell_{min} = 6$ .

#### 4.2.3 $f(\ell) = \ell$

$\ell_{max} = 22 \rightarrow 30$  for  $avg_e$  are anomalous for COMM, with the maximal s-value being 96.01% for  $\ell_{max} = 26$ .  $\ell_{min} = 6$  for  $max_e$  is anomalous with an s-value of 97.05%, whereas  $\ell_{min} = 2$  is anomalous at an s-value of 95.73% for  $avg_e$  for COMM. There are no anomalies

for NILC for variations in  $\ell_{max}$ . For  $\ell_{min} = 6$ , there is a 96.88% s-value for  $max_e$  and 98.51% for  $avg_e$  respectively for NILC. For SMICA,  $\ell_{max} = 22 \rightarrow 30$  are anomalous with maximal s-value being 95.87% for  $\ell_{max} = 26$ .  $\ell_{min} = 6$  with 97.10% s-value for  $max_e$  shows anomalous behaviour for SMICA, while  $\ell_{min} = 2, 6$  for  $avg_e$  with  $\ell_{min} = 6$  of maximal s-value of 97.50% show anomalous behaviour. For WMAP, there is a change, because it shows that  $\ell_{max} = 6, 10$  for  $min_o$  are anomalous with maximal s-value of 98.99% for  $\ell_{max} = 6$ .  $\ell_{max} = 10, 14$  are anomalous for  $min_e$  with maximal s-value of 98.24% for  $\ell_{max} = 10$ . Also for WMAP,  $\ell_{max} = 10 \rightarrow 30$  are anomalous for  $avg_e$  with maximal s-value of 98.15% for  $\ell_{max} = 26$ .  $\ell_{min} = 6, 10$  are anomalous for  $max_e$  for WMAP, but  $\ell_{min} = 6$  is most anomalous with an s-value of 99.77%. Again,  $\ell_{min} = 2, 6$  are anomalous for  $avg_e$  but  $\ell_{min} = 6$  is most anomalous with an s-value of 99.14%. [See figure 8].

#### 4.2.4 $f(\ell) = \ell^2$

In this case, COMM does not have anomalies for  $\ell_{min}$  variations.  $\ell_{max} = 6 \rightarrow 14$  are anomalous for  $min_e$  for COMM, being maximally anomalous for  $\ell_{max} = 6$  with an s-value of 99.15%. For NILC,  $\ell_{max} = 22 \rightarrow 30$  are anomalous for  $avg_e$  with  $\ell_{max} = 26$  being maximally anomalous with an s-value of 97.14%.  $\ell_{min} = 6 \rightarrow 14$  are anomalous for  $max_e$  for NILC, with a maximal s-value of 98.23% for  $\ell_{min} = 10$ .  $\ell_{min} = 2 \rightarrow 10$  are also anomalous for  $avg_e$  with a maximal s-value of 96.79% for  $\ell_{min} = 6$  for NILC. For SMICA,  $\ell_{max} = 18 \rightarrow 30$  are anomalous with maximal s-value of 97.68% for  $\ell_{max} = 26$  for  $avg_e$ . Also,  $\ell_{min} = 10$  is anomalous for  $max_o$  with s-value of 97.29% for SMICA.  $\ell_{min} = 6, 10$  are anomalous for  $max_e$  with  $\ell_{min} = 6$  being of maximal s-value of 97.30%, whereas for  $avg_e$ ,  $\ell_{min} = 2, 6$  are anomalous with maximal s-value of 96.48% for  $\ell_{min} = 2$ . For WMAP, again,  $\ell_{max} = 18 \rightarrow 30$  are all anomalous for  $min_o$ , but  $\ell_{max} = 18$  is most anomalous with an s-value of 98.23%. Also, for WMAP,  $\ell_{max} = 14 \rightarrow 30$  are all anomalous for  $avg_e$ , but  $\ell_{max} = 26$  is most anomalous with an s-value of 99.60%.  $\ell_{min} = 2 \rightarrow 14$  are anomalous for  $min_o$  with a maximal s-value of 97.26% for  $\ell_{min} = 14$  for WMAP, whereas, for the even separations of WMAP's  $\ell^2 C_\ell$ 's,  $\ell_{min} = 6$  with an s-value of 96.51% is anomalous for  $max_e$ , while,  $\ell_{min} = 2 \rightarrow 10$  are all anomalous for  $avg_e$ , but  $\ell_{min} = 2$  is most anomalous with an s-value of 98.38%. [See figure 9].

## 5 Summary

### 5.1 All multipole separations

We realise that on restricting the anomalous ranges as those corresponding to or beyond 99.7% as the s-value of a simulation being errant relative to observational data, which implies a nearly equal to or greater than  $3\sigma$  confidence for an anomaly (see table 1 for all  $\gtrsim 3\sigma$  anomalies), we can sieve out the maximally anomalous results. The most significantly anomalous  $\ell_{min} = 8$  has a maximal proba-

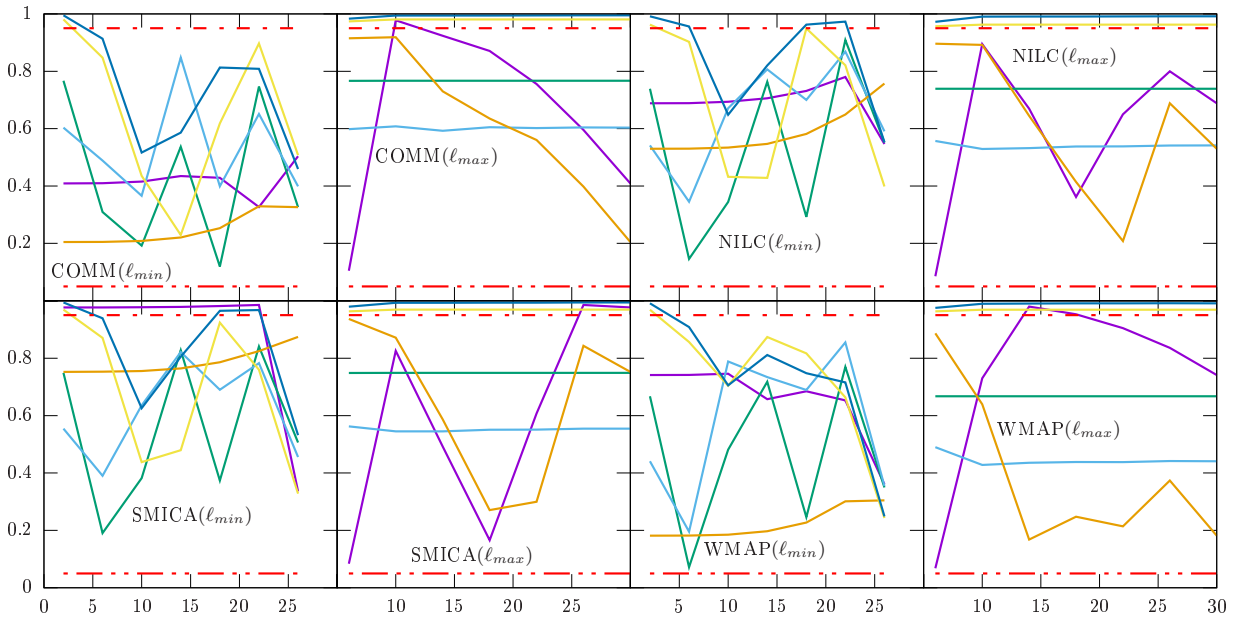


Figure 6: Probabilities  $P^t$  for  $min_o$ ,  $max_o$ ,  $avg_o$ ,  $min_e$ ,  $max_e$ ,  $avg_e$  (in purple, green, light blue, ochre, yellow and dark blue) for  $f(\ell) = 1$  versus  $\ell_{max}$  or  $\ell_{min}$  as mentioned in parentheses () beside the name of the data map. Red dotted-dashed lines indicate 5% (double dots) and 95% (single dots).

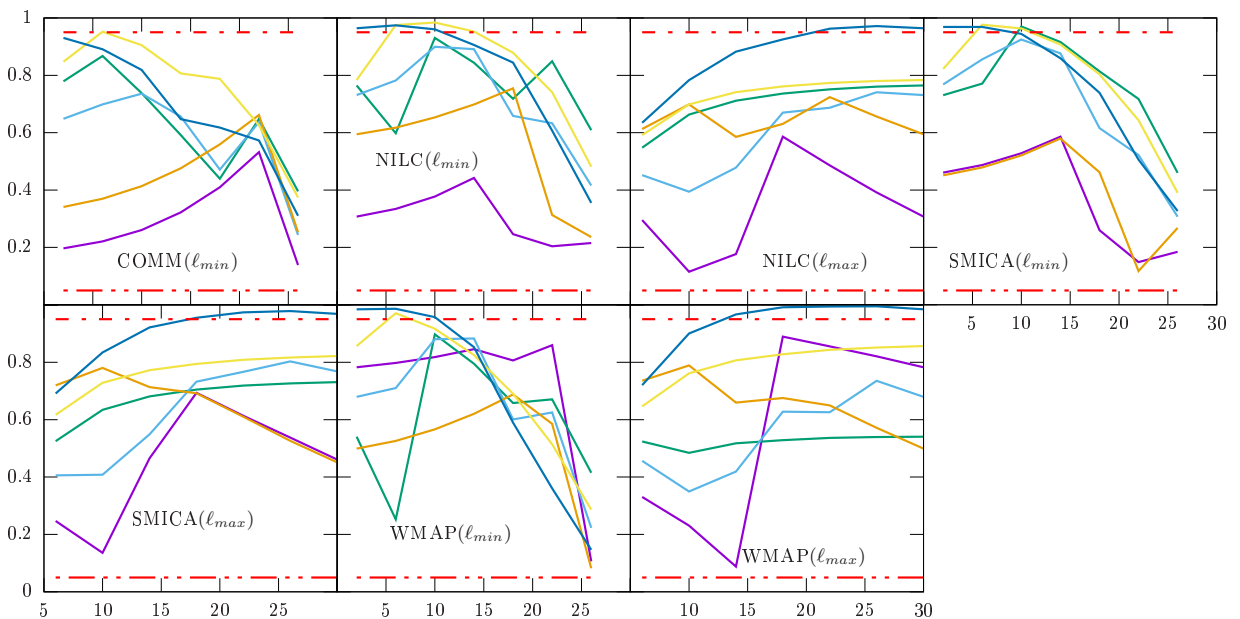


Figure 7: Probabilities  $P^t$  for  $min_o$ ,  $max_o$ ,  $avg_o$ ,  $min_e$ ,  $max_e$ ,  $avg_e$  (in purple, green, light blue, ochre, yellow and dark blue) for  $f(\ell) = \frac{\ell(\ell+1)}{2\pi}$  versus  $\ell_{max}$  or  $\ell_{min}$  as mentioned in parentheses () beside the name of the data map. Red dotted-dashed lines indicate 5% (double dots) and 95% (single dots).

bility for NILC (for  $f(\ell) = \frac{\ell(\ell+1)}{2\pi}$ ) of 99.93% and also for WMAP (for  $f(\ell) = \ell$ ) of 99.93%, both for the maximum separations of the respective  $f(\ell)C_\ell$ 's. These correspond to  $\approx 3.4\sigma$  deviant anomalies. For the average separations, the maximal probabilities are shown by NILC for  $f(\ell) = \frac{\ell(\ell+1)}{2\pi}$ ,  $\ell_{min} = 8$  with value of 99.7%, and also shown by WMAP for  $f(\ell) = \ell$ ,  $\ell_{min} = 8$ , with value 99.78%. Again for  $\ell_{max} = 26$ , the most significantly anomalous are NILC and SMICA, both for maximum separation with probabilities of 99.78% and 99.89% respectively. So mainly, the maximum separation turns out to

be anomalous with highest s-values (lowest p-values) for  $\ell_{min} = 8$  and  $\ell_{max} = 26$ . These anomalies at a significance  $\approx 3.25\sigma$  are highlighted in table 1.

We further present the plots of p-values (in log-scale along the vertical axis), which are those of the probabilities  $P^b$ , and  $P^b = 1 - P^t$ . These plots give a better insight on the extent to which the observational data are deviant from the theoretical predictions, indicated by the lowermost dips in the plots of figure 10.

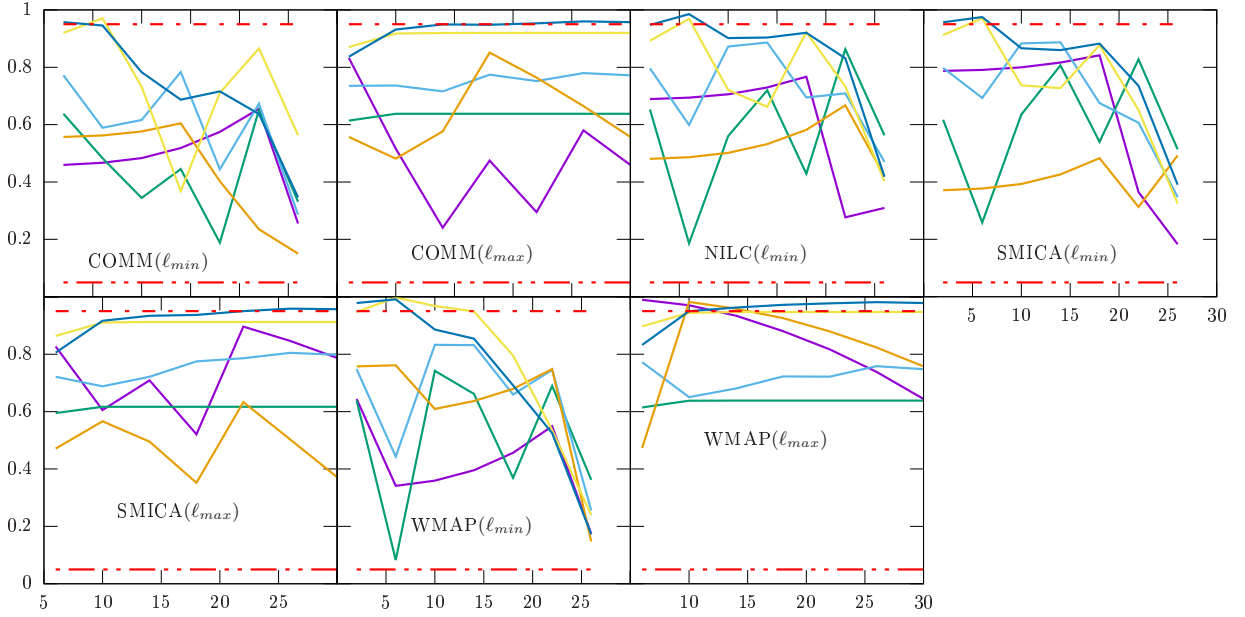


Figure 8: Probabilities  $P^t$  for  $min_o, max_o, avg_o, min_e, max_e, avg_e$  (in purple, green, light blue, ochre, yellow and dark blue) for  $f(\ell) = \ell$  versus  $\ell_{max}$  or  $\ell_{min}$  as mentioned in parentheses () beside the name of the data map. Red dotted-dashed lines indicate 5% (double dots) and 95% (single dots).

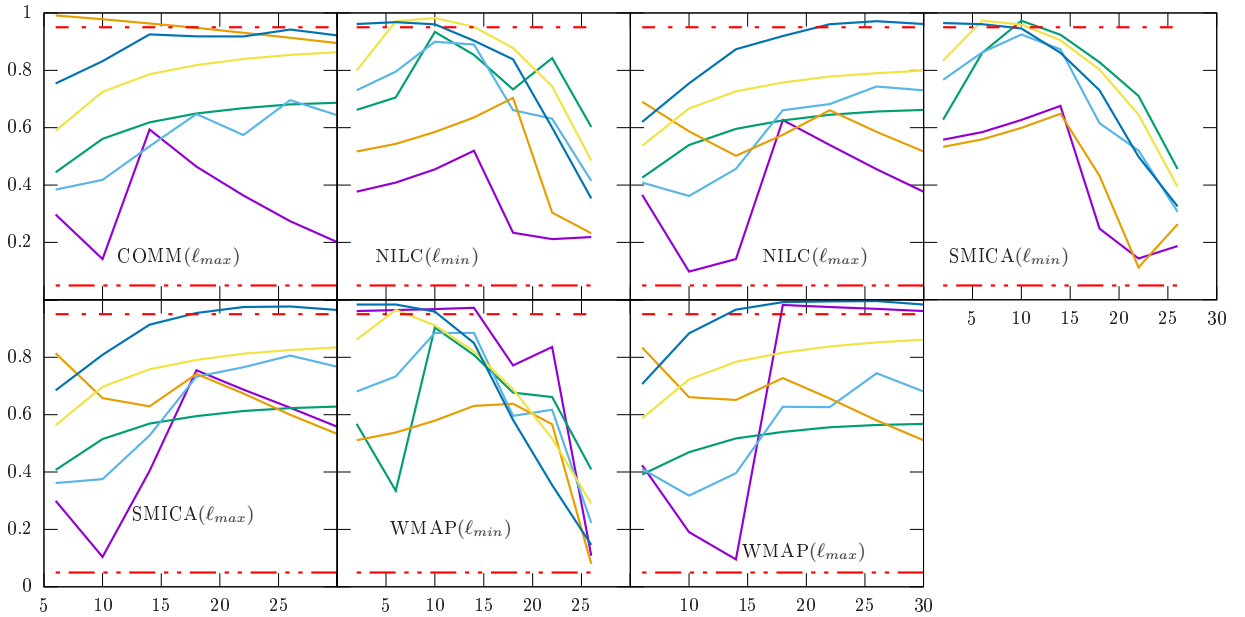


Figure 9: Probabilities  $P^t$  for  $min_o, max_o, avg_o, min_e, max_e, avg_e$  (in purple, green, light blue, ochre, yellow and dark blue) for  $f(\ell) = \ell^2$  versus  $\ell_{max}$  or  $\ell_{min}$  as mentioned in parentheses () beside the name of the data map. Red dotted-dashed lines indicate 5% (double dots) and 95% (single dots).

## 5.2 Odd/even multipole separations

On glancing at the most essentially anomalous ranges, we realise that there is only one  $\gtrsim 3\sigma$  anomaly (shown by WMAP) : 99.77% for  $\ell_{min} = 6$  for  $max_e$  (when  $f(\ell) = \ell$ ). We present the most significant anomalies for  $\gtrsim 2.75\sigma$  range (corresponding to a confidence range  $\gtrsim 99.40\%$ ) in the tables in 2 that follow and wherein the  $\gtrsim 3\sigma$  anomaly has been highlighted.

The general trend (of  $\gtrsim 2.5\sigma$  anomalies) however, seems to hold for that of  $avg_e$  being anomalous for all maps for  $f(\ell) = 1$ , with high (above 99%) probability for  $\ell_{min} = 2$

and  $\ell_{max} = 26$  and/or 30. Further, for  $f(\ell) = \frac{\ell(\ell+1)}{2\pi}$  there is an isolated anomaly again for  $avg_e$  with  $\ell_{max} = 26$  for WMAP. WMAP dominates these ‘highly significant’ anomalies for  $f(\ell) = \ell$ , for  $\ell_{max} = 6$  for  $min_o$  (which doesn’t appear for other  $f(\ell)$ ’s, at this level of significance), and  $\ell_{min} = 6$  for  $max_e$  and  $avg_e$ . For  $f(\ell) = \ell^2$ , COMM has an anomaly for  $\ell_{max} = 6$  for  $min_e$ , while WMAP shows that for  $\ell_{max} = 22, 26$  for  $avg_e$ .

An overall impression from the results is that the even separations show up as anomalies for most of the maps; the odd separations are seldom anomalous in as much as their

Table 1:  $\gtrsim 3\sigma$  anomalies for **all** separations (with  $\gtrsim 3.25\sigma$  results highlighted)

$$f(\ell) = \frac{\ell(\ell+1)}{2\pi}$$

Data Map	$\ell_{min}$ or $\ell_{max}$	Type	s-value ( $P^t$ )
COMM	$\ell_{min} = 8$	$Max_a$	<b>99.88%</b>
NILC	$\ell_{min} = 8$	$Max_a$	<b>99.93%</b>
NILC	$\ell_{min} = 10$	$Max_a$	99.75%
NILC	$\ell_{min} = 8$	$Avg_a$	99.70%

$$f(\ell) = \ell$$

Data Map	$\ell_{min}$ or $\ell_{max}$	Type	s-value ( $P^t$ )
NILC	$\ell_{min} = 8$	$Max_a$	99.72%
SMICA	$\ell_{min} = 8$	$Max_a$	99.86%
SMICA	$\ell_{min} = 8$	$Avg_a$	99.72%
WMAP	$\ell_{min} = 8$	$Max_a$	<b>99.93%</b>
WMAP	$\ell_{min} = 8$	$Avg_a$	99.78%

$$f(\ell) = \ell^2$$

Data Map	$\ell_{min}$ or $\ell_{max}$	Type	s-value ( $P^t$ )
COMM	$\ell_{min} = 8$	$Max_a$	99.83%
NILC	$\ell_{min} = 8$	$Max_a$	<b>99.91%</b>
NILC	$\ell_{min} = 10$	$Max_a$	99.70%

maximum, minimum and average value are concerned. Besides, in the most significant results for anomalies as presented in the table 2, it is evident that the average value of separations among odd  $f(\ell)C_\ell$ 's, i.e.,  $avg_o$  is never anomalous. For the odd separations,  $min_o$  is anomalous for  $\ell_{max} = 6$  with a 98.99% probability only for WMAP and only for  $f(\ell) = \ell$ . The average separation among even multipoles ( $avg_e$ ), is always anomalous for all  $f(\ell)$ 's, but shows up selectively in the various data maps for the respective  $f(\ell)$ 's. Among the  $\gtrsim 2.5\sigma$  significant results,  $max_e$  also shows up only once for  $f(\ell) = \ell$ . For this case, where parity based differentiation is done before the separations are analysed, there are multiple anomalous ranges for the four maps and for all the four  $f(\ell)$ 's because a wider confidence interval is taken ( $\gtrsim 2.75\sigma$ ). The p-value plots for the same are presented in figure 11.

## 6 Results: Separation ratios

In addition to checking solely for anomalous separations, we also checked if the ratio ( $r_i$ ) of the maximum to the minimum separation (as defined in (3)) of a given range of multipoles is anomalous. The s-value plots of the most significantly anomalous results are presented in figure 12, which show that SMICA is not very problematic for sep-

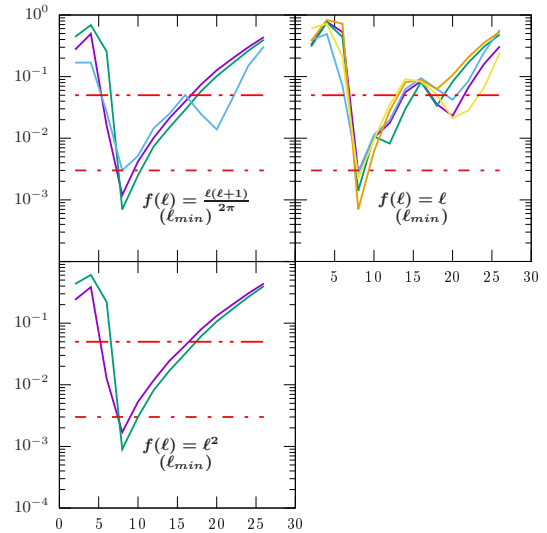


Figure 10: Plots of p-values ( $P^b$ ) versus  $\ell_{min}$  or  $\ell_{max}$  as indicated in parentheses (), for  $\gtrsim 3\sigma$  anomalies for all separations. Top left: COMM ( $max_a$ ) in purple, NILC ( $max_a$ ) in green, NILC ( $avg_a$ ) in light blue. Top right: NILC ( $max_a$ ) in purple, SMICA ( $max_a$ ) in green, SMICA ( $avg_a$ ) in light blue, WMAP ( $max_a$ ) in ochre, WMAP ( $avg_a$ ) in yellow. Bottom left: COMM ( $max_a$ ) in purple, NILC ( $max_a$ ) in green. Dotted-dashed red lines represent: 5% ( $\sim 2\sigma$ ) (above) and 0.3% ( $\sim 3\sigma$ ) (below).

aration ratios sans parity distinction. Although the other three maps show most anomalous ratios, yet COMM and WMAP most recurrently show anomalies in as much as all, odd and even multipole separation ratios are concerned.

The anomalous ratios of highest significance in each of the four subplots of figure 12 are (clockwise from top) : (1) COMM for  $r_a$ ,  $f(\ell) = 1$  with an s-value of 98.66% at  $\ell_{min} = 22$ , (2) WMAP for  $r_a$ ,  $f(\ell) = 1$  with an s-value of 97.25% at  $\ell_{max} = 22$ , (3) SMICA for  $r_o$ ,  $f(\ell) = 1$  with a p-value of 98.49% at  $\ell_{min} = 6$  and, (4) COMM for  $r_e$ ,  $f(\ell) = \ell^2$  with a p-value of 99.3% at  $\ell_{max} = 6$ .

The  $\ell_{min}$  and  $\ell_{max}$  ranges are similar to those which turned up as anomalous when only separations were considered. Besides,  $r_e$  is anomalous at the highest significance, which agrees with most of the previous analyses that showed how even multipole separations are at a dissonance with theoretical simulations.

## 7 Digression: ‘Parity asymmetry’ mitigation

In the review article [28], the authors using the concept of constructing symmetric and antisymmetric functions for the temperature field (that have even and odd parity respectively), emphasise the notion of how a significant power asymmetry between even and odd multipoles may be interpreted as a preference for a particular parity of the anisotropy pattern, referred to as ‘parity asymmetry’. They use a ratio of the following two constructed measures to

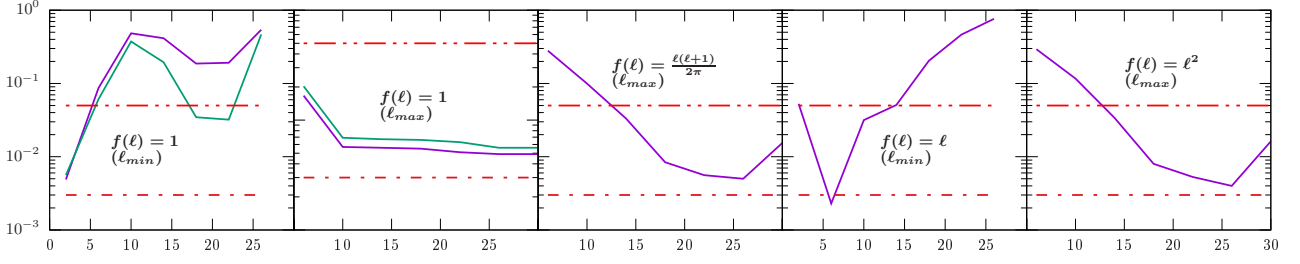


Figure 11: Plots for p-values ( $P^b$ ) versus  $\ell_{min}$  or  $\ell_{max}$  as indicated in parentheses (), for  $\gtrsim 2.75\sigma$  anomalies for even and odd multipole separations. Top left: COMM ( $avg_e$ ) in purple, SMICA ( $avg_e$ ) in green. Top right: COMM ( $avg_e$ ) in purple, SMICA ( $avg_e$ ) in green. Middle left: WMAP ( $avg_e$ ) in purple. Middle right: WMAP ( $max_e$ ) in purple. Bottom left: WMAP ( $avg_e$ ) in purple. Dotted-dashed red lines represent: 5% ( $\sim 2\sigma$ ) (above) and 0.3% ( $\sim 3\sigma$ ) (below).

Table 2:  $\gtrsim 2.75\sigma$  anomalies for **odd/even** separations (with  $\gtrsim 3\sigma$  results highlighted)

$f(\ell) = 1$			
Data Map	$\ell_{min}$ or $\ell_{max}$	Type	s-value ( $P^t$ )
COMM	$\ell_{max} = 26, 30$	$Avg_e$	99.51%
COMM	$\ell_{min} = 2$	$Avg_e$	99.51%
SMICA	$\ell_{max} = 26, 30$	$Avg_e$	99.44%
SMICA	$\ell_{min} = 2$	$Avg_e$	99.44%
$f(\ell) = \frac{\ell(\ell+1)}{2\pi}$			
Data Map	$\ell_{min}$ or $\ell_{max}$	Type	s-value ( $P^t$ )
WMAP	$\ell_{max} = 22$	$Avg_e$	99.44%
WMAP	$\ell_{max} = 26$	$Avg_e$	99.50%
$f(\ell) = \ell$			
Data Map	$\ell_{min}$ or $\ell_{max}$	Type	s-value ( $P^t$ )
WMAP	$\ell_{min} = 6$	$Max_e$	<b>99.77%</b>
$f(\ell) = \ell^2$			
Data Map	$\ell_{min}$ or $\ell_{max}$	Type	s-value ( $P^t$ )
WMAP	$\ell_{max} = 22$	$Avg_e$	99.47%
WMAP	$\ell_{max} = 26$	$Avg_e$	99.60%

test this ‘parity asymmetry’:

$$\begin{aligned}
 P^+ &= \sum_{\ell=\ell_{min}}^{\ell_{max}} \cos^2\left(\frac{\ell\pi}{2}\right) f(\ell)C_\ell \\
 P^- &= \sum_{\ell=\ell_{min}}^{\ell_{max}} \sin^2\left(\frac{\ell\pi}{2}\right) f(\ell)C_\ell
 \end{aligned} \quad (5)$$

with  $f(\ell) = \frac{\ell(\ell+1)}{2\pi}$  only and test the same only for WMAP data for the 3, 5 and 7 year releases and fixed  $\ell_{min} = 2$ .

We test the same for six  $f(\ell)$ 's, i.e.,  $f(\ell) =$

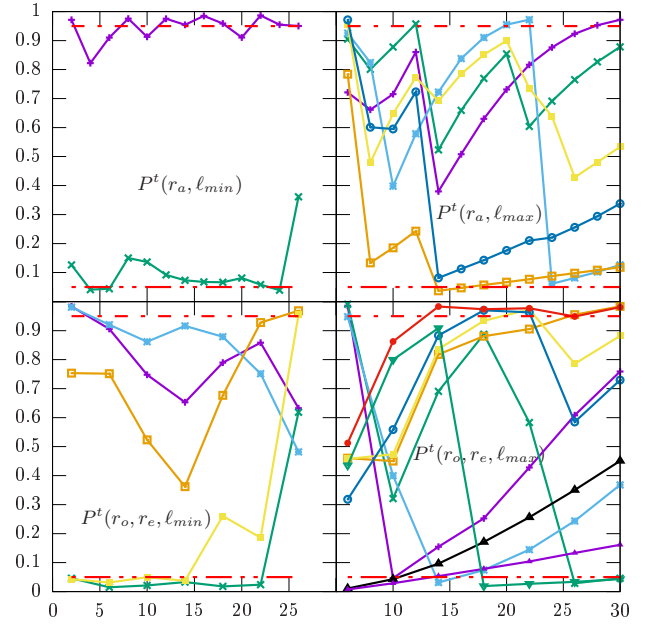


Figure 12: Anomalous ratios of maximum to minimum separations: Probabilities  $P^t(r_i)$ ,  $i = a, o, e$  versus  $\ell_{max}$  or  $\ell_{min}$  as mentioned in parentheses (). Top left: COMM, WMAP for  $f(\ell) = 1$  in purple and green, respectively. Top right: COMM, NILC, WMAP for  $f(\ell) = 1$  in purple, green and light blue, respectively; NILC for  $f(\ell) = \frac{\ell(\ell+1)}{2\pi}$  in ochre; NILC, WMAP for  $f(\ell) = \ell$  in yellow and dark blue, respectively. Bottom left: COMM ( $r_e$ ), SMICA ( $r_o$ ), WMAP ( $r_e$ ) for  $f(\ell) = 1$  in purple, green and light blue, respectively; COMM ( $r_e$ ) for  $f(\ell) = \ell$  in ochre; WMAP ( $r_o$ ) for  $f(\ell) = \ell^2$  in yellow. Bottom right: COMM ( $r_o$ ), SMICA ( $r_o$ ), WMAP ( $r_o$ ), COMM ( $r_e$ ), NILC ( $r_e$ ), SMICA ( $r_e$ ), WMAP ( $r_e$ ) for  $f(\ell) = 1$  in purple (+), green ( $\times$ ), light blue, ochre, yellow, dark blue and red, respectively; WMAP ( $r_o$ ) for  $f(\ell) = \ell$  in black; COMM ( $r_e$ ), WMAP ( $r_o$ ) for  $f(\ell) = \ell^2$  in purple ( $\blacktriangle$ ) and green ( $\nabla$ ), respectively. Red dotted-dashed lines indicate 5% (double dots) and 95% (single dots).

1,  $\frac{\ell(\ell+1)}{2\pi}$ ,  $\ell$ ,  $\ell^2$ ,  $\ell^3$ ,  $\ell^4$  and for four maps [Planck 2018 maps of COMM, NILC, SMICA and WMAP 9 year ILC (1)]. We also vary  $\ell_{min}$  from  $2 \rightarrow 28$  and  $\ell_{max}$  from  $4 \rightarrow 30$ , both in steps of  $\Delta\ell = 2$ . And also our definition of  $\ell_{max}$  is slightly different: we denote  $\ell_{max} = 6$  for  $\ell \in [2, 7]$ , etc. When  $\ell_{min}$  is varied,  $\ell_{max}$  is fixed at 30, i.e., the range

$\ell_{min} \leq \ell \leq 31$  is considered. Whereas, when  $\ell_{max}$  is varied,  $\ell_{min}$  is fixed at 2.

Comparing the ratio  $\frac{P^+}{P^-}$  from these observed data maps with the same evaluated from  $10^4$  simulations generated from the theoretical best fit to Planck, we perform our familiar p-value analysis as discussed in (3). To reiterate, p-value = Number of simulations having  $\frac{P^+}{P^-}$  lesser than that from data. A low  $\frac{P^+}{P^-}$  indicates an odd-parity preference, which has been shown by several authors ([10], [42], [29], [3]). This translates to a low p-value, and the lower the p-value, the more significant is the anomaly. Works of [10], [42], [29], [3], show that  $f(\ell) = \frac{\ell(\ell+1)}{2\pi}$  is still problematic for the low multipoles  $< 30$ .

Our analysis reveals that as we approach higher powers of  $\ell$  in  $f(\ell)$ , the p-values rise much above the 5% ( $\sim 2\sigma$ ) and 0.3% ( $\sim 3\sigma$ ) red lines, as can be seen for  $f(\ell) = \ell^3, \ell^4$  for both  $\ell_{min}$  and  $\ell_{max}$  variations; although for  $\ell_{min}$  variations, the anomalies completely disappear for these  $f(\ell)$ 's, which is why we have not tested  $f(\ell) = \ell^3, \ell^4$  in our analysis of separations (3, 4.1, 4.2). All the p-value plots are in figure 13.

*These plots indicate that the most significant p-value in both cases ( $\ell_{min}$  and  $\ell_{max}$  variations) is that of WMAP for  $f(\ell) = \frac{\ell(\ell+1)}{2\pi}$ , given by  $\ell_{min} = 2$  with p-value = 0.0094 and  $\ell_{max} = 24$  with p-value = 0.008, respectively. Our lowest p-values are different from [28], because we have taken equal number of even and odd multipoles for each computation of  $\frac{P^+}{P^-}$ , by ensuring  $\Delta\ell = 2$ , whereas [28] have apparently taken  $\Delta\ell = 1$ . p-values of lower significance for WMAP are  $\ell_{max} = 24, 26$  (for  $f(\ell) = 1$ ),  $\ell_{max} = 22, 26$  (for  $f(\ell) = \ell$ ),  $\ell_{max} = 24$  (for  $f(\ell) = \ell^2$ ),  $\ell_{max} = 6$  (for  $f(\ell) = \ell^3, \ell^4$ ) and  $\ell_{min} = 2$  (for  $f(\ell) = 1, \ell, \ell^2$ ).*

Planck maps also show a highly recurrent anomalous  $\ell_{max} = 6$  (for  $f(\ell) = \frac{\ell(\ell+1)}{2\pi}, \ell^2, \ell^3, \ell^4$ ),  $\ell_{max} = 8$  (for  $f(\ell) = 1, \ell$ ) and  $\ell_{min} = 2$  (for  $f(\ell) = 1$  for COMM,  $f(\ell) = 1, \frac{\ell(\ell+1)}{2\pi}, \ell$  for NILC and SMICA, and  $f(\ell) = \ell^2$  for NILC). COMM, however does not show anomalies for  $\ell_{max}$  variations for  $f(\ell) = \ell^4$ . NILC reveals an anomalous  $\ell_{max} = 24$  for  $f(\ell) = \ell$ .

As we approach higher powers of  $\ell$  as aforementioned, the p-values tend to recede back into our 5%–95% confidence range and the anomalies are obscured.  $\ell_{min} = 2$  is most recurrently anomalous, which indicates that as soon as we change the lower limit to exclude the quadrupole (or use higher powers of the multipole:  $f(\ell) = \ell^3, \ell^4$ ), the anomalies cease to exist in the case of  $\ell_{min}$  variations for all four data maps, and this is congruent with earlier studies that have pointed out how anomalously low is the power associated with the quadrupole ([37], [36], [4], [24], [39]). However, as opposed to Planck maps which show this effect with low significance, WMAP shows this anomaly at high significance.

This analysis gives us a cue to use  $f(\ell)$  with higher powers of the multipole to alleviate the problems of the anomalous parity asymmetry. This is also the reason why we have used a set of such four simple  $f(\ell)$ 's while trying to find anomalous separations in  $f(\ell)C_\ell$ 's as our 'tested power spectra' because in a similar vein, [12] describes how using a function as a multiplicative factor to the temperature field can be used to explain some large-scale anomalies.

## 8 Conclusions

We have proposed a new technique for investigating anomalies in the CMB temperature angular power spectrum for its nearest neighbour separations and found that such anomalous separations arise in various multipole ranges, across all four data maps, with a variation of the lower or upper limit of the multipole range or a change in an  $f(\ell)$ . In this section, we will try to deliberate on some obvious trends.

Reasonably, since all four maps, namely, COMM, NILC, SMICA, and WMAP, have been obtained by using different foreground removal methods, the levels of foreground residuals in these maps are quite different ([31], [2], [18]). These systematic differences are clearly visible if we subtract any two of these maps at low resolution. Therefore, since each cleaned map is obtained by using different foreground filters, the residual foreground in each of them is expected to be different. This can be a possible cause of different results obtained from differently cleaned maps [36].

The p-value plots in figure 10, show that for all separations, for  $\ell_{min} = 8$  and  $\ell_{max} = 26$ , the maximum separation from theoretical predictions is most significantly greater than that from observations for all  $f(\ell)$ 's except  $f(\ell) = 1$ . For odd and even parity based distinctions, p-value plots in figure 11, reveal how  $\ell_{min} = 6$  and  $\ell_{max} = 22$  are the most anomalous because in these  $\ell$  ranges, the maximum separation among  $f(\ell)C_\ell$ 's for even  $\ell$ 's from theoretical simulations is mostly larger than observed data.  *$P^t = 99.93\%$  is the highest probability among all the p-values in all our analyses, and is exhibited by  $\ell_{min} = 8$  for all (no parity distinction) multipole separations for  $f(\ell) = \frac{\ell(\ell+1)}{2\pi}$  for NILC and  $f(\ell) = \ell$  for WMAP.*

Initially, a low quadrupole anisotropy was reported ([37], [11]), and shown to be a part of the general trend of parity asymmetry [28]. *We too, observe that lower  $\ell_{min}$ 's seem to be more anomalous and after a certain  $\ell_{min}$  value is crossed, the anomalies disappear, most conspicuously for our analysis of parity asymmetry in section 7.*

Parity based distinction reveals that *the even multipoles have a more significant tendency to keep their maximum separations much smaller than what is theoretically predicted.* Also a noticeable feature of the Planck maps (COMM, NILC, SMICA) is that without any parity based distinction, the minimum separation does not usually show up as an anomaly. However, when the odd and even multipoles are considered separately, the minimum separation for odd multipoles begins to show up as being anomalously lower than theoretical simulations (especially for  $f(\ell) = 1$ ), whereas, the maximum of even separations is almost always anomalously low and at relatively much higher significance. This anomaly disappears for higher powers of  $\ell$  in  $f(\ell)$  (except for  $f(\ell) = \ell, \ell^2$  in WMAP). This implies that the very low maximum separations of even multipoles override the effect of possibly low odd multipole separations in  $f(\ell)C_\ell$ 's when all multipoles are studied without any parity based distinctions.

Our analyses here clearly spell out that for all multipole separations taken without parity based distinction,  $f(\ell) = 1$  is not excluded at as high a significance as the others. *Only for NILC, and WMAP,  $f(\ell) = \ell, \frac{\ell(\ell+1)}{2\pi}$  are excluded*

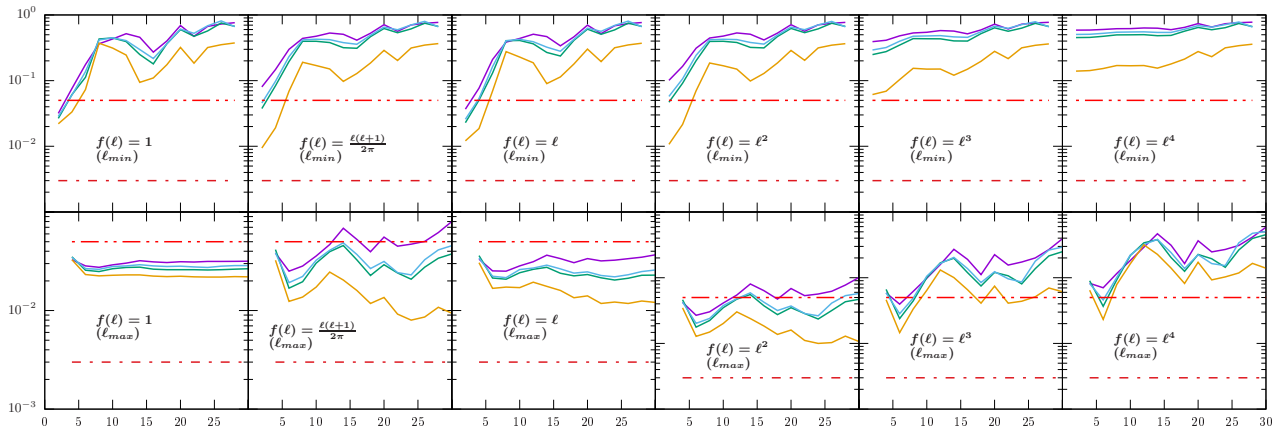


Figure 13: p-value versus  $\ell_{min}$  or  $\ell_{max}$  as indicated in parentheses () for mitigating parity asymmetry with  $f(\ell)$  (section 7). Coloured lines are representative of the four maps : COMM (purple), NILC (green), SMICA (light blue), WMAP (dark yellow). Dotted red lines represent: 5% ( $\sim 2\sigma$ ) (above) and 0.3% ( $\sim 3\sigma$ ) (below). Higher powers of  $\ell$  in  $f(\ell)$  tend to mitigate the anomalies better.

at the  $3.4\sigma$  significance level for  $max_a$  in the multipole range  $8 \leq \ell \leq 31$ , which indicate strong deviations from the traditional Sachs-Wolfe plateau and from  $f(\ell) = \ell$ , respectively. For odd and even multipole separations treated distinctly, WMAP excludes  $f(\ell) = \ell$  with  $3.05\sigma$  significance in the range  $6 \leq \ell \leq 31$  for the maximum even multipole spectrum separation. Thus,  $f(\ell) = \ell, \ell^2, \frac{\ell(\ell+1)}{2\pi}$  are most significantly excluded for all separations, while  $f(\ell) = 1$  is excluded at relatively lower significance; but for the even multipole spectrum,  $f(\ell) = \ell$  is excluded at a higher significance relative to  $f(\ell) = 1, \ell^2, \frac{\ell(\ell+1)}{2\pi}$ .

The anomalous behaviour of specific multipole ranges and the even multipole separations is consistent with the analysis of separation ratios in section (6). We must note however, that all these results are specific to certain maps as aforementioned and all the four maps show sundry anomalies with high significance. Hence, this precludes the possibility of such a clear conclusion about the rejection of  $f(\ell)$ 's for separations in the temperature power spectrum. Besides, we need a more succinct characterisation of why higher order  $f(\ell)$ 's should work for mitigating the parity asymmetry anomaly (7). A study of the physical origin of these anomalies may constitute a work in the future.

## Acknowledgements

We acknowledge some initial use of the HEALPix [25] software package which is publicly available (<http://healpix.sourceforge.io>). Our analyses are based on observations obtained with Planck (<http://www.esa.int/Planck>), an ESA science mission with instruments and contributions directly funded by ESA Member States, NASA, and Canada. We acknowledge the use of the Legacy Archive for Microwave Background Data Analysis (LAMBDA), part of the High Energy Astrophysics Science Archive Center (HEASARC). HEASARC/LAMBDA is a service of the Astrophysics Science Division at the NASA Goddard Space Flight Center. MIK would like to thank Ujjal Purkayastha for immense help in guiding him through the basics of HEALPix relevant to this project.

## References

- [1] L. Raul Abramo, Laerte Sodré, and Carlos Alexandre Wuensche. Anomalies in the low cmb multipoles and extended foregrounds. *Phys. Rev. D*, 74:083515, Oct 2006.
- [2] Peter Ade, N. Aghanim, Charmaine Armitage-Caplan, M. Arnaud, Mark Ashdown, F. Atrio-Barandela, Jonathan Aumont, Carlo Baccigalupi, A. Banday, Ramon Barreiro, J. Bartlett, E. Battaner, K. Benabed, A. Benoît, Aurélien Benoit-Lévy, J.-P Bernard, M. Bersanelli, P. Bielewicz, J. Bobin, and A. Zonca. Planck 2013 results. xii. component separation. *Astronomy and Astrophysics*, 571, 03 2013.
- [3] Pavan K. Aluri and Pankaj Jain. Parity asymmetry in the CMBR temperature power spectrum. *Monthly Notices of the Royal Astronomical Society*, 419(4):3378–3392, 01 2012.
- [4] C. L. Bennett, M. Halpern, G. Hinshaw, N. Jarosik, A. Kogut, M. Limon, S. S. Meyer, L. Page, D. N. Spergel, G. S. Tucker, E. Wollack, E. L. Wright, C. Barnes, M. R. Greason, R. S. Hill, E. Komatsu, M. R. Nolte, N. Odegard, H. V. Peiris, L. Verde, and J. L. Weiland. First-year wilkinson microwave anisotropy probe ( WMAP ) observations: Preliminary maps and basic results. *The Astrophysical Journal Supplement Series*, 148(1):1–27, sep 2003.
- [5] A. Bernui, A.F. Oliveira, and T.S. Pereira. North-south non-gaussian asymmetry in Planck CMB maps. *Journal of Cosmology and Astroparticle Physics*, 2014(10):041–041, oct 2014.
- [6] Helge Blaker. Confidence curves and improved exact confidence intervals for discrete distributions. *Canadian Journal of Statistics*, 28(4):783–798, 2000.
- [7] Martin Bucher. Physics of the cosmic microwave background anisotropy. *Int. J. Mod. Phys.*, D24(02):1530004, 2015.

- [8] Alexander Gallego Cadavid, Antonio Enea Romano, and Stefano Gariazzo. Cmb anomalies and the effects of local features of the inflaton potential. *The European Physical Journal C*, 77(4):242, Apr 2017.
- [9] Zhe Chang, Pranati K Rath, Yu Sang, Dong Zhao, and Yong Zhou. Finsler space–time can explain both parity asymmetry and power deficit seen in CMB temperature anisotropies. *Monthly Notices of the Royal Astronomical Society*, 479(1):1327–1331, 06 2018.
- [10] Cheng Cheng, Wen Zhao, Qing-Guo Huang, and Larissa Santos. Preferred axis of cmb parity asymmetry in the masked maps. *Physics Letters B*, 757:445 – 453, 2016.
- [11] Lung-Yih Chiang, Pavel D. Naselsky, and Peter Coles. Cosmic Covariance and the Low Quadrupole Anisotropy of the Wilkinson Microwave Anisotropy Probe (WMAP) Data. *Mod. Phys. Lett. A*, 23:1489–1497, 2008.
- [12] Craig J. Copi, Dragan Huterer, Dominik J. Schwarz, and Glenn D. Starkman. Large angle anomalies in the CMB. *Adv. Astron.*, 2010:847541, 2010.
- [13] M. Cruz, L. Cayon, E. Martinez-Gonzalez, P. Vielva, and J. Jin. The non-gaussian cold spot in the 3 Year-Wilkinson microwave anisotropy ProbeData. *The Astrophysical Journal*, 655(1):11–20, jan 2007.
- [14] M. Cruz, E. Martínez-González, P. Vielva, and L. Cayón. Detection of a non-Gaussian spot in WMAP. *Monthly Notices of the Royal Astronomical Society*, 356(1):29–40, 01 2005.
- [15] Santanu Das and Tarun Souradeep. Suppressing CMB low multipoles with ISW effect. *JCAP*, 02:002, 2014.
- [16] Angélica de Oliveira-Costa, Max Tegmark, Matias Zaldarriaga, and Andrew Hamilton. Significance of the largest scale cmb fluctuations in wmap. *Phys. Rev. D*, 69:063516, Mar 2004.
- [17] Angelica de Oliveira-Costa, Max Tegmark, Matias Zaldarriaga, and Andrew Hamilton. The Significance of the largest scale CMB fluctuations in WMAP. *Phys. Rev. D*, 69:063516, 2004.
- [18] H. K. Eriksen, A. J. Banday, K. M. Górski, and P. B. Lilje. On Foreground Removal from the Wilkinson Microwave Anisotropy Probe Data by an Internal Linear Combination Method: Limitations and Implications. *The Astrophysics Journal*, 612(2):633–646, September 2004.
- [19] European Space Agency. Planck Legacy Archive. <https://pla.esac.esa.int/#maps>, 2018.
- [20] R.A. Fisher. *Statistical methods for research workers*. Edinburgh Oliver & Boyd, 1925.
- [21] D. J. Fixsen. THE TEMPERATURE OF THE COSMIC MICROWAVE BACKGROUND. *The Astrophysical Journal*, 707(2):916–920, nov 2009.
- [22] Caroline L. Francis and John A. Peacock. An estimate of the local integrated Sachs-Wolfe signal and its impact on cosmic microwave background anomalies. *Monthly Notices of the Royal Astronomical Society*, 406(1):14–21, July 2010.
- [23] Mayukh R. Gangopadhyay, Grant J. Mathews, Kiyotomo Ichiki, and Toshitaka Kajino. Explaining low  $\ell$  anomalies in the CMB power spectrum with resonant superstring excitations during inflation. *Eur. Phys. J. C*, 78(9):733, 2018.
- [24] E. Gaztañaga, J. Wagg, T. Multamäki, A. Montaña, and D. H. Hughes. Two-point anisotropies in WMAP and the cosmic quadrupole. *Monthly Notices of the Royal Astronomical Society*, 346(1):47–57, 11 2003.
- [25] K. M. Górski, E. Hivon, A. J. Banday, B. D. Wandelt, F. K. Hansen, M. Reinecke, and M. Bartelmann. HEALPix: A Framework for High-Resolution Discretization and Fast Analysis of Data Distributed on the Sphere. *The Astrophysics Journal*, 622(2):759–771, April 2005.
- [26] A. Gruppuso, N. Kitazawa, M. Lattanzi, N. Mandolesi, P. Natoli, and A. Sagnotti. The Evens and Odds of CMB Anomalies. *Phys. Dark Univ.*, 20:49–64, 2018.
- [27] G. Hinshaw, D. N. Spergel, L. Verde, R. S. Hill, S. S. Meyer, C. Barnes, C. L. Bennett, M. Halpern, N. Jarosik, A. Kogut, E. Komatsu, M. Limon, L. Page, G. S. Tucker, J. L. Weiland, E. Wollack, and E. L. Wright. First-YearWilkinson microwave anisotropy probe(WMAP) observations: The angular power spectrum. *The Astrophysical Journal Supplement Series*, 148(1):135–159, sep 2003.
- [28] Kim, Jaiseung, Naselsky, Pavel, Hansen, and Martin. Symmetry and antisymmetry of the cmb anisotropy pattern, Aug 2012.
- [29] Jaiseung Kim and Pavel Naselsky. ANOMALOUS PARITY ASYMMETRY OF THEWILKINSON MICROWAVE ANISOTROPY PROBEPOWER SPECTRUM DATA AT LOW MULTIPOLES. *The Astrophysical Journal*, 714(2):L265–L267, April 2010.
- [30] Kate Land and João Magueijo. Is the universe odd? *Phys. Rev. D*, 72:101302, Nov 2005.
- [31] D. Larson, J. L. Weiland, G. Hinshaw, and C. L. Bennett. COMPARINGPLANCKANDWMAP: MAPS, SPECTRA, AND PARAMETERS. *The Astrophysical Journal*, 801(1):9, feb 2015.
- [32] Richard D Morey, Rink Hoekstra, Jeffrey N Rouder, Michael D Lee, and Eric-Jan Wagenmakers. The fallacy of placing confidence in confidence intervals, Feb 2016.
- [33] National Aeronautics and Space Administration. WMAP 9 year ILC map. [https://lambda.gsfc.nasa.gov/product/map/dr5/ilc\\_map\\_get.cfm](https://lambda.gsfc.nasa.gov/product/map/dr5/ilc_map_get.cfm), 2012.

- [34] J. Neyman. Outline of a Theory of Statistical Estimation Based on the Classical Theory of Probability. *Phil. Trans. Roy. Soc. Lond.*, A236(767):333–380, 1937.
- [35] C Pernet. Null hypothesis significance testing: a guide to commonly misunderstood concepts and recommendations for good practice [version 5; peer review: 2 approved, 2 not approved]. *F1000Research*, 4(621), 2017.
- [36] A. Rassat, J. L. Starck, P. Paykari, F. Sureau, and J. Bobin. Planck CMB anomalies: astrophysical and cosmological secondary effects and the curse of masking. *Journal of Cosmology and Astroparticle Physics*, 2014(8):006, August 2014.
- [37] Dominik J Schwarz, Craig J Copi, Dragan Huterer, and Glenn D Starkman. CMB anomalies after Planck. *Classical and Quantum Gravity*, 33(18):184001, aug 2016.
- [38] Dominik J. Schwarz, Glenn D. Starkman, Dragan Huterer, and Craig J. Copi. Is the low- $l$  microwave background cosmic? *Phys. Rev. Lett.*, 93:221301, 2004.
- [39] Max Tegmark, Angelica de Oliveira-Costa, and Andrew Hamilton. A high resolution foreground cleaned CMB map from WMAP. *Phys. Rev. D*, 68:123523, 2003.
- [40] P. Vielva, E. Martinez-Gonzalez, R. B. Barreiro, J. L. Sanz, and L. Cayon. Detection of non-gaussianity in the Wilkinson microwave anisotropy Probe First-year data using spherical wavelets. *The Astrophysical Journal*, 609(1):22–34, jul 2004.
- [41] Michael Wood. P values, confidence intervals, or confidence levels for hypotheses? *arXiv e-prints*, page arXiv:0912.3878, December 2009.
- [42] Wen Zhao. Directional dependence of cmb parity asymmetry. *Phys. Rev. D*, 89:023010, Jan 2014.